Mechanical state assessment using lamb wave technique in static tensile tests

M V Burkov[1,2], R T Shah[1], A V Eremin[1,2], A V Byakov[1,2], S V Panin[1,2]
[1]Institute of High Technology Physics, National Research Tomsk Polytechnic University, 634050, Lenina ave 30, Tomsk, Russia
[2]ISPMS SB RAS, 634021, Akademicheskiy ave 2/4, Tomsk, Russia

E-mail: burkovispms@mail.ru

Abstract. The paper deals with the investigation of Lamb wave ultrasonic technique for damage (or mechanical state) evaluation of AA7068T3 specimens in the course of tensile testing. Two piezoelectric transducers (PZT), one of which is used as an actuator and the other as sensor, were adhesively bonded on the specimen surface using epoxy. Two frequencies of testing signals (60 kHz and 350 kHz) were used. The set of static tensile tests were performed. The recorded signals were processed to calculate the informative parameters in order to evaluate the changes in stress-strain state of the specimens and their microstructure.

1. Introduction

The modern non-destructive testing (NDT) techniques are used in manufacturing and in-service inspection to ensure product integrity and reliability, as well as to control of manufacturing processes in order to reduce the production costs while maintaining high quality. During construction, NDT is used to monitor the uniformity of materials, welded joints, etc., while in-service NDT inspections are used to confirm that the products in use continue to have the integrity necessary to provide the sufficient reliability [1].

The emerging trend in the field of inspection during operation is to increase the NDT performance allowing saving time as well as fund. Thus over the past several decades, a significant research efforts have been focused on Structural Health Monitoring (SHM). The SHM concept is based on the use of in-situ non-destructive sensing and analysis of structural characteristics including the structural response in order to detect changes that may indicate damage or degradation. The output of SHM process is periodically updated informing about the ability of the structure to continue performing its intended function in the light of the inevitable aging and damage accumulation caused by the operational environments. Under an extreme event, such as an earthquake or unanticipated blast loading, SHM is used for rapid condition screening. This screening is intended to provide, in near real-time, reliable information about system performance during such extreme events and the subsequent integrity of the system [2, 3].

All active SHM operations require the development of complex algorithms and software for data processing and continuation of operation decision-making [4, 5]. The basis for the software is a deformation, damage accumulation and fracture mechanics of different materials. To test designed system and software the joint consideration of experimental data and computer modelling is required. There are a lot of papers dealing with research of ultrasonic systems utilizing Lamb wave principle and algorithms for damage detection. However, in most of them the PZTs without substrate are used.

Such PZTs will be inappropriate for cyclic loading during operation due to brittleness and low ultimate stress of piezoceramics. The aim of the present work is to assess the applicability of PZTs with steel substrate for damage evaluation as well as to investigate the response of the actuator-sensor pairs on different stress-strain state of the loaded aluminum specimens. The experimental results of ultrasonic examination using Lamb waves of AA7068T3 specimens tested with static tension are presented in the paper.

2. Materials and technique

The investigated ultrasonic technique was applied for evaluation of AA7068 specimens' mechanical state during static uniaxial tensile testing. The specimens were cut in the dogbone shape (figure 1) from the 4 mm sheet. The specimens were split on two groups: the first was used for testing in the initial state; the specimens from the second group were cut across gage length and then welded using gas tungsten arc welding. The AW1E12G-190EFL1Z piezoelectric discs used as transducers were adhesively bonded to the surface using 3M Scotch Weld DP105.

The ultrasonic technique used during tensile testing is described in details in [6]. There was a 100 signals averaging used to increase S/N ratio. Then the informative parameters (Maximum Envelope [7], Normalized Correlation Coefficient NCC and Variance μ_2) were calculated in order to associate the stress-strain state evolution with characteristic changes of propagated ultrasonic signal.
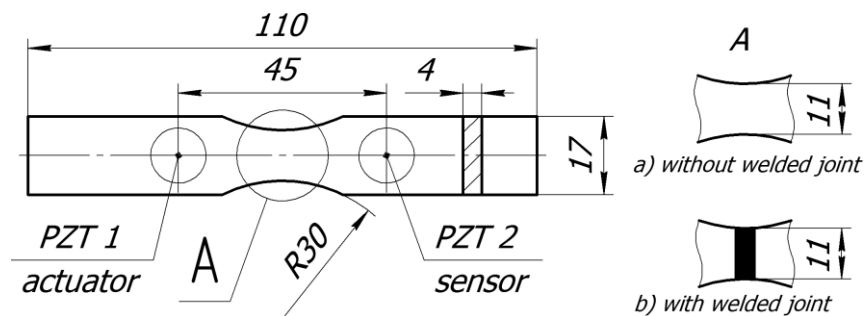

Figure 1. The sketch of the specimen with the PZTs on the specimen surface.

The static tensile testing was carried out using electromechanical testing machine Instron 5582 with the strain rate of 0.6 mm/min. The loading was stopped in defined points for capturing of ultrasonic data (the specimen was fixed in grips and subjected to tensile load). During the elastic region the step of 1 kN by load was used, when the plasticity started the step was changed to 0.2 % of elongation. So the dependence of the recoded signal amplitude on the stress-strain state was studied. The main goal of the static tests is to investigate the response of the actuator-sensor pairs during loading and to ensure the possibility of PZTs and epoxy adhesive application for further fatigue evaluation tests of the AA7068 specimens.

During each tensile test the strain and stress values were captured using gages of the Instron testing machine while the specimen was imaged using the Vic-3D digital image correlation (DIC) system. DIC system allowed us to obtain strain values calculated from the surface of the deformed specimen. This data can be used as the additional source of strain information during analysis of results.

3. Results and discussion

The preliminary study was carried out in order to choose the appropriate frequency for further testing: the actuator-sensor response of the specimen fixed in grips was characterized by the dependence (figure 2) in terms of maximum envelope of the signal versus ultrasound frequency. The frequency was varied in the range from 10 to 400 kHz with the step of 1 kHz. It is easily seen from the figure 2 that there are three main peaks of the maximum envelope corresponding to the frequencies of 60 kHz, 150 kHz and 350 kHz. The dispersion curves for aluminum plates obtained experimentally and theoretically [8-10] allow calculating the group velocities and the wavelengths of A_0 and S_0 modes for the specimens with thickness of 4 mm. Thus the first peak at 60 kHz corresponds to the high

amplitude of A_0 mode while the amplitude of S_0 is negligible because it has long wavelength at this frequency. The third peak (350 kHz) corresponds to the S_0 mode. The second peak at ~150 kHz is also associated with the mix of mainly A_0 and S_0. Actually the association of these peaks with different modes of Lamb waves is calculated with an error about 5-15 % in comparison with the theoretical values. This discrepancy is related to the different boundary conditions of the specimen which is fixed in grips as well as due to its small size where side reflections can greatly change the signal sensed by the receiver.
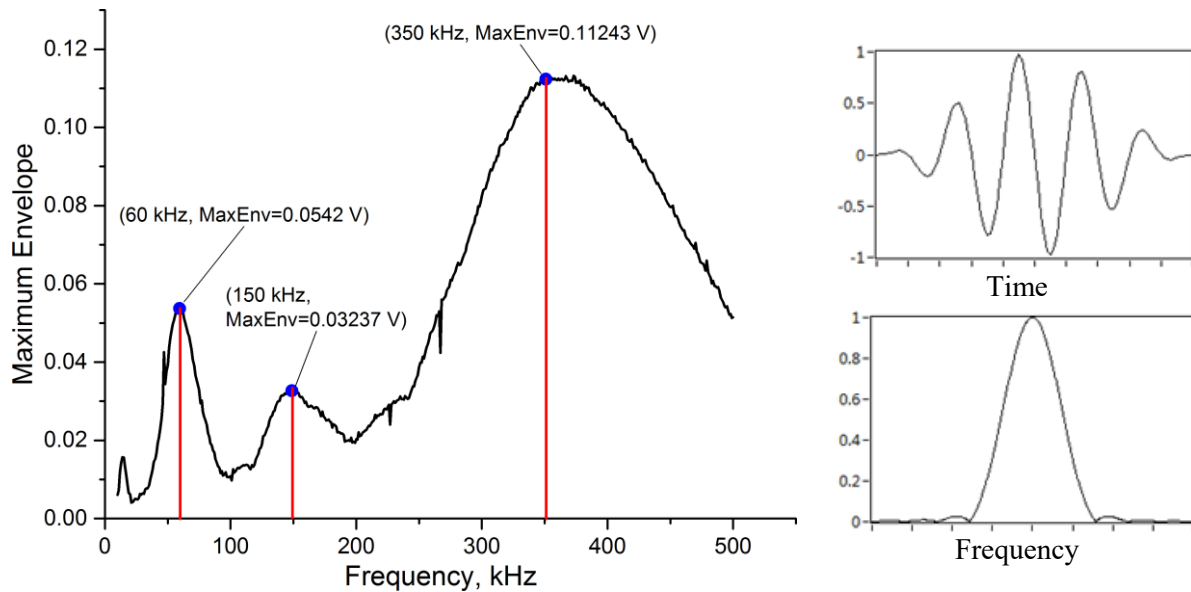

Figure 2. The dependence of the sensed signal amplitude on the frequency.
The examples of the signal in time and frequency domains are shown.

This work deals with the investigation of the possibility of ultrasonic technique to characterize the changes in the specimen dimensions due to the deformation as well as microstructural changes of the material in the highly stressed gage length. Due to higher magnitude the first and the third peaks corresponding to the actuating frequency of 60 and 350 kHz were used during tensile testing. Thus the A_0 mode of Lamb waves was generated using low frequency scanning signal while S_0 mode with higher group velocity was generated at high frequency.
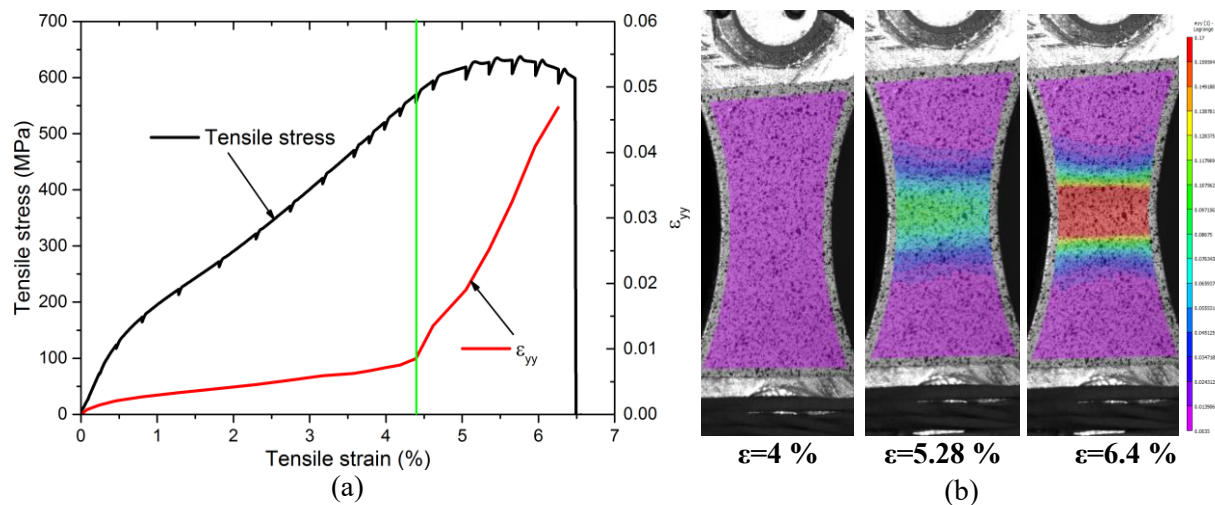

Figure 3. The stress-strain curve for the step mode tension test of the AA7068 specimen (a) and normal strain ε_{yy} measured by the Vic-3D (b).

Figure 3a represents the stress-strain curve of the AA7068 specimen loaded in step mode until fracture: there are 21 points of defined loads and strains where loading was stopped and ultrasound testing was performed. It could be observed that the vertical green line divides the graph on Figure 3 onto the elastic region and the region with plastic deformation where the specimen is deformed irreversibly. The ε_{yy} graph was plotted by averaging of all ε_{yy} values in the calculation area shown on Figure 3b. The ε_{yy} plot is also divided on two stages. The first stage is characterized by the fully elastic straining of the specimen and the images of ε_{yy} field look nearly uniform while at the second stage the plasticity concentrates in the narrowest cross section of the specimen thus the ε_{yy} plot rises rapidly.
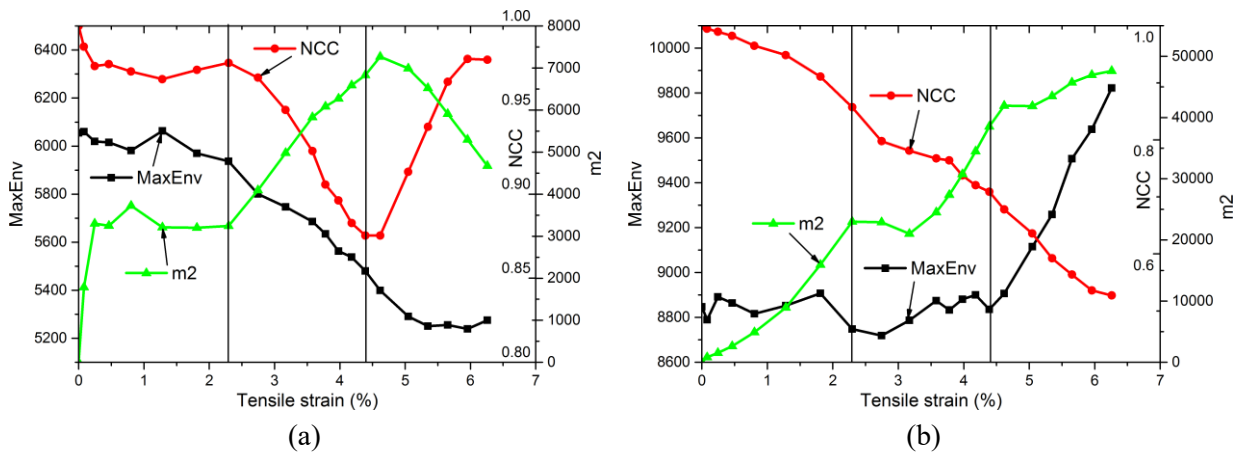

Figure 4. The plots of maximum of envelope (MaxEnv), normalized correlation coefficient (NCC) and variance μ_2 (m2) by the elongation for initial AA7068 specimen: (a) 60 kHz and (b) 350 kHz.

Figure 4 displays the interdependence between informative parameters and applied strain. For low frequency the max of envelope (MaxEnv) is decreasing during all straining process until fracture with a small region during plasticity where the values remain nearly constant. This change can be associated with the slight variation of the specimen dimensions due to elongation thus the Lamb waves arrive to the sensor at different phase with a wave reflected from boundaries and different interference pattern occurs.
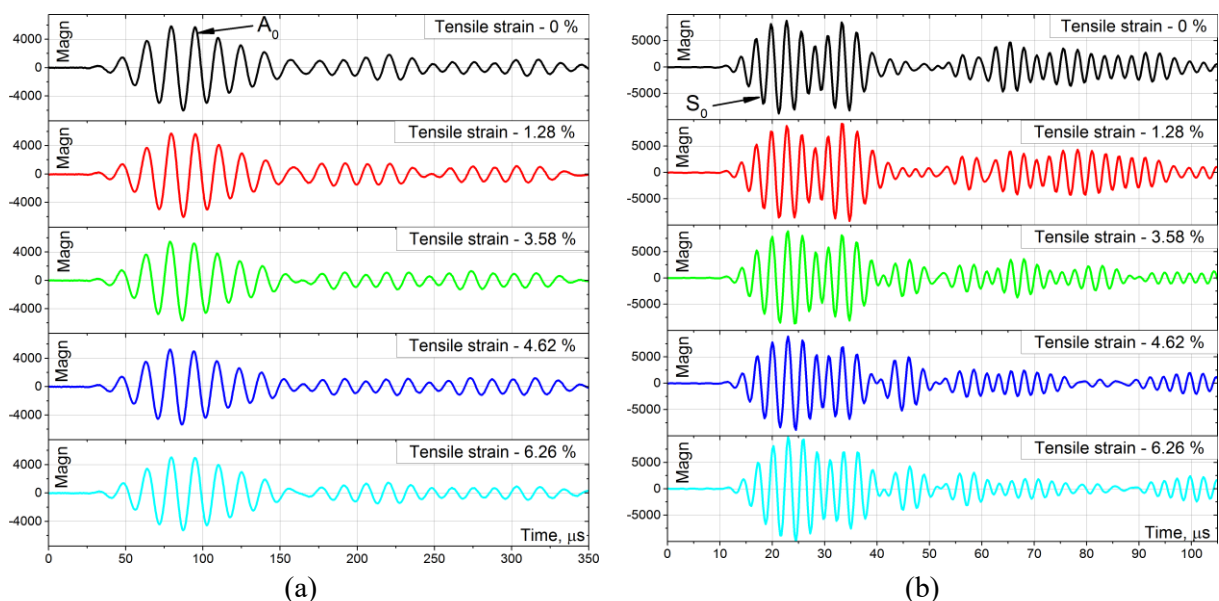

Figure 5. The images of signal waveforms captured for the specimen without welded joint
(a) 60 kHz, (b) 350 kHz.

Two parameters characterizing the waveform changes of the signals (Variance μ_2 and NCC) have nearly the same behavior (considering their reverse nature – the higher the differences of compared signals the higher the μ_2, while NCC will be lower). Such relation is relevant to all of the sets of results presented in the paper so only the NCC parameter will be described and discussed. As for the figure 4a the normalized correlation coefficient after the first stage with constant values decreases but during plastic deforming it goes back thus just before the fracture the NCC is nearly the same as at the beginning of the tensile test. Such controversial result doesn't allow us to make a correct decision on the state of the specimen thus it should be concluded that entirely the low frequency testing provides not reliable results. The informative parameters obtained for the high frequency of testing signal (figure 4b) have a better explainable behavior: the NCC decreases during the entire tensile test while the MaxEnv stays nearly constant until the plastic deformation starts (after 4.4 % elongation).
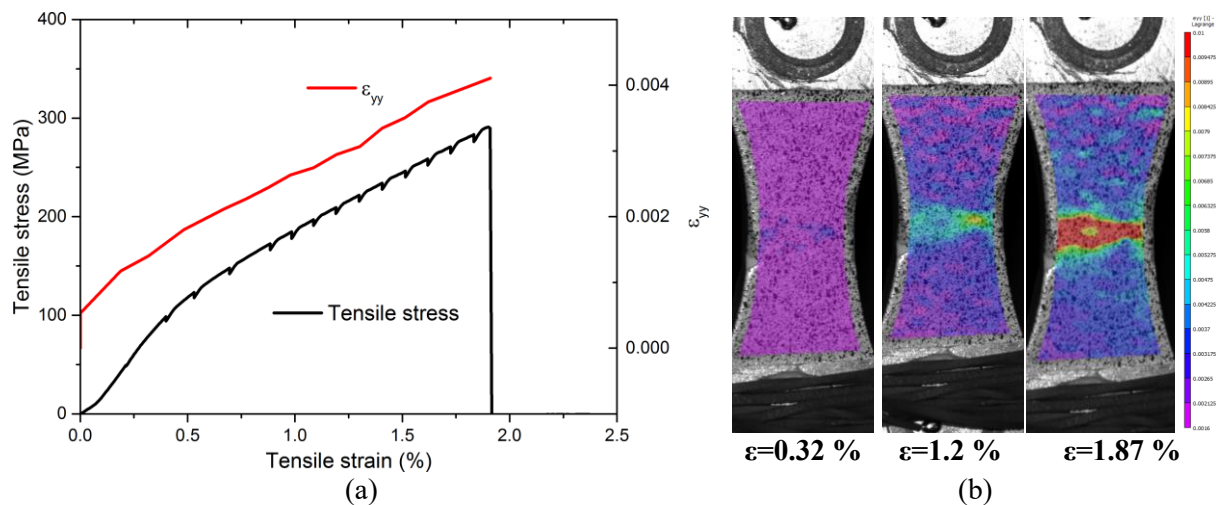

Figure 6. The stress-strain curve for the step mode tension test of the welded AA7068 specimen (a) and normal strain ε_{yy} measured by Vic-3D (b).

Figure 5 shows the images of signal waveforms recorded during the tensile test. By the joint analysis of the informative parameters and these plots we can highlight the following regularities: (1) the shape of the first wave packet of low frequency signals is almost unchanged during the test, there are only a minor changes of the signals' "tail"; (2) a close look to the first wave packet figure 5a indicates that the amplitude of received signals decreases that is confirmed by the MaxEnv plot; (3) the first wave packet of the high frequency signal (which corresponds to the S_0 mode) stays nearly unchanged and the MaxEnv increases on the last stage as well; (4) the second wave packet is produced most likely by the side reflections and decrease significantly during the test; (5) the "tail" of the high frequency sensed signals changes drastically throughout the tensile test, but it is quite difficult to make any precise assumption about this due to small size of the specimen and large amount of different reflected waves that interfere with each other.

It can be seen in figure 6 that the welded joint drastically decreases the ultimate strength: σ_u of initial AA7068 alloy is about 627 MPa while for the specimen with welded joint the fracture point is at 290 MPa. Actually this alloy has low weldability by methods of liquid state welding like tungsten arc welding. Present work is aimed on the investigation of the ultrasonic testing technique thus high mechanical properties do not have a significant importance. Instead this weakened welded joint acts like a strain concentrator that can be seen from the stress-strain and ε_{yy} curves. While the specimen without welded joint has two easily identified stages of the ε_{yy} curve due to good plasticity of initial material the ε_{yy} curve for welded specimen is linear showing nearly elastic deformation behavior and brittle fracture. The area of welded joint at fracture exhibits elastic strains due to the lack of plasticity of welded material thus the averaged ε_{yy} curve is nearly linear.

Figure 7 shows the graphs of the informative parameters for the frequency of 60 kHz and 350 kHz. Due to low weldability of AA7068 the specimen fractured at low elongations (within 2-2.5 % of elongation). This leads to the lower stressed state of the specimen just before the fracture compared to the non-welded specimen.
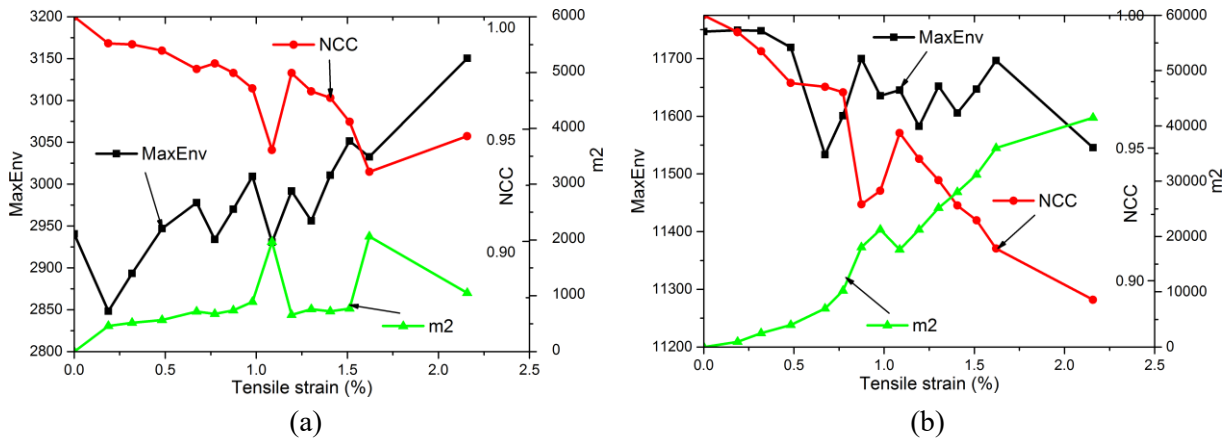

Figure 7. The plots of maximum of envelope (1), normalized correlation coefficient (2) and variance μ_2 (3) by the elongation for welded AA7068 specimen: (a) 60 kHz and (b) 350 kHz.

The analysis of the data gives the following conclusion: the behavior of the plots of the informative parameters for the welded specimen is nearly the same as for the first stage for the initial specimen without welding joint (this stage is shown by the vertical black line on figure 4). For the high frequency testing the MaxEnv stays nearly the same until fracture and NCC decreases during the entire tensile test. For the low frequency all informative parameters have a sideway trend.
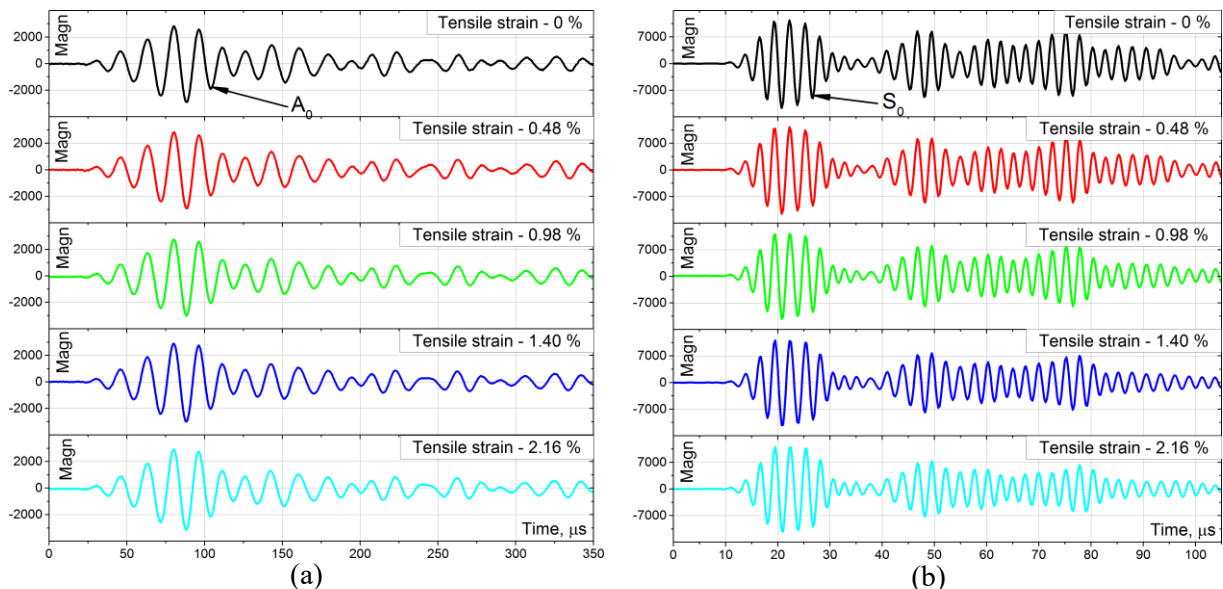

Figure 8. The images of signal waveforms captured for the specimen with welded joint (a) 60 kHz, (b) 350 kHz and for the specimen with welded joint.

Figure 8 shows the variations of captured signals throughout the tensile test of specimen with welded joint. The shapes of signals compared to those for the specimen without welded joint are nearly the same. In the low frequency plots the A_0 mode is easily distinguished and its shape doesn't changes up to fracture. The "tail" of the signal at 60 kHz also stays constant up to fracture. For the high frequency the first wave packet corresponds to S_0 mode but now the second wave packet is observed separately

from the S_0. It confirms the assumption that this wave packet can be associated to the interference of side reflections. Also it can be seen that the signal "tail" has higher amplitude in comparison with the initial specimen signal waveforms.

4. Conclusion

The static tensile tests of AA7068 specimens were performed with acquisition of strain data using Instron load and strain gages, strain distribution fields via VIC-3D system and ultrasonic data by acoustic inspection system. After the digital processing of raw acoustic signal data, the set of informative parameters was calculated including MaxEnv and NCC characterizing the changes in propagated signal amplitude and its shape correspondingly. After the analysis of the results we can conclude the following:

1) Small size of the specimen leads to the very complex and inexplicable results. There are a lot of boundary reflections from sides of the specimen as well as the influence of grips of testing machine which is very difficult to assess.

2) It is seen that low frequency testing (using A_0 mode of Lamb waves) doesn't provide good results of quantitative analysis of signals. High frequency tests (mainly S_0 mode) provide better explainable results allowing it to be used for characterizing the changes of stress-strain state of the specimen during loading.

3) The first wave packet of the signal for all specimens was used to calculate the MaxEnv parameter, while the entire signal was analyzed by NCC and Variance μ_2. But according to the plots (figure 4) the last parameters allow to make better conclusions about the state of the specimen. Thus it is necessary to make a more detailed investigation of variation of the shape of the first wave packet of sensed signal, because now NCC and Variance μ_2 are influenced by the "tail" of the signal which behavior is difficult to explain in contrast to the first travelled wave packet which is less influenced by the side reflections and grips.

References

[1]   Hellier C 2001 *Handbook of Nondestructive Evaluation* (New York: McGraw-Hill Professional) 594 p
[2]   Diamanti K, Soutis C 2010 *Prog. Aerosp. Sci.* **46** 342–352
[3]   Farrar C, Worden K 2007 *Phil. Trans. R. Soc. A.* **365** 303–315
[4]   R. Kazys, O. Tumsys, D. Pagodinas 2008 *NDT&E Int.* **41** 457–466
[5]   Torres-Arredondo M, Tibaduiza D, Mujica L, Rodellar J and Fritzen C-P 2014 *Struct. Health Monit.* **13** 19-32
[6]   Burkov M, Byakov A, Shah R, Lyubutin P and Panin S 2015 *IOP Conf. Series.* **93** 012025
[7]   Hahn SL 1996 *Hilbert Transforms in Signal Processing* Norwood, USA, Artech House, 460 p
[8]   Giurgiutiu V, Cuc A 2005 *Shock. Vib. Digest.* **37** 783-105
[9]   Hyun Woo P, Seung Bum K, Hoon S 2009 *Wave Motion* **46** 451–467
[10] Cho H and Lissenden CJ 2012 *Struct. Health Monit.* **11** 393-404